Thermal conductivity of Y-junction carbon nanotubes

Aron Cummings,[1,*] Mohamed Osman,[1,†] Deepak Srivastava,[2] and Madhu Menon[3]
[1]*School of Electrical Engineering and Computer Science, Washington State University, Pullman, Washington 99164, USA*
[2]*NASA Ames Research Center, MST27A-1, Moffett Field, California 94035, USA*
[3]*Department of Physics and Astronomy and Center for Computational Sciences University of Kentucky, Lexington, Kentucky 40506, USA*
(Received 17 March 2004; published 8 September 2004)

The thermal conductivity of a Y-junction carbon nanotube with a (14,0) trunk splitting into two (7,0) branches has been investigated using a molecular dynamics approach. It has been found that the thermal conductivity of the Y-junction nanotube is less than that of a corresponding straight (14,0) nanotube, due to lattice defects in the form of nonhexagonal carbon rings at the junction. These lattice defects result in a discontinuity in the temperature profile of the Y-junction nanotube. Defects that were introduced to a straight (14,0) nanotube resulted in a similar discontinuity in the temperature profile.

DOI: 10.1103/PhysRevB.70.115405 PACS number(s): 65.80.+n

I. INTRODUCTION

Since their discovery in 1991,[1] carbon nanotubes have been a subject of great interest among the scientific research community. This interest has been sparked by the emerging field of nanotechnology, which focuses on the construction of useful devices whose sizes are on the nanometer scale. Over the past decade, much work has been done on the characterization of these nanotubes. Theoretical studies of their electrical properties have indicated that the nanotubes can be either metallic or semiconducting.[2] In addition, it was found that that the band gap of the semiconducting nanotubes is inversely proportional to the nanotube radius.[3] The diameter-dependence of the band gap of the semiconducting nanotubes has led researchers to propose and investigate a variety of structures that involve the connection of one nanotube to another. Based on the topology of five- and seven-member ring defects and quantum molecular dynamics simulations to validate the stability, three-terminal T- and Y-junctions of carbon nanotubes were proposed through modeling and simulation-based approaches.[4–6] Y-junctions of multiwall carbon nanotubes were then fabricated using a template based approach that allows the fabrication of many Y-junctions in a single experiment.[7,8] Since then, many other experimental approaches have been developed and have reported the formation of multiwall carbon nanotube Y-, H-, and X-junctions in a variety of experimental conditions. See, for example, Ref. 6 for a review of the developments in this area. Three-terminal T- and Y-junctions, and four-terminal X-junctions of single-wall carbon nanotubes have also recently become feasible in ion-beam induced welding of carbon nanotubes.[9]

Enabled by various growth and fabrication techniques, experimental work has revealed some interesting electrical properties of these Y-junction nanotubes. The electronic current versus voltage (*I-V*) characteristics have been measured[7,8] and simulated,[10,11] and show that the three-terminal branched carbon nanotubes exhibit rectifying behavior, with current flowing more easily when a negative bias is applied to the trunk or base of the junction.[6–11] Recent theoretical studies of the Y-junction nanotube have helped to further elucidate the rectifying nature of the Y-branched structure.[10,11] In these studies, quantum conductance calculations are made to determine the *I-V* characteristics of a variety of configurations of the Y-junction nanotube. It is concluded that both the symmetry of the Y-junction and the chirality of the trunk and branches play a role in the rectification behavior of these structures, with the symmetry being a more significant factor. In this paper we investigate the thermal conductivity of Y-junction carbon nanotubes using a molecular dynamics simulation approach, so that similar questions can be answered about the thermal transport behavior in these structures. The details and results of this approach are discussed in Secs. I and III, respectively.

II. METHODOLOGY

To model the dynamics of the atoms within the Y-junction nanotube, a molecular dynamics (MD) approach has been chosen, with the Tersoff-Brenner bond order potential for the C-C bond as the potential interaction function.[12,13] Within the MD paradigm, a variety of approaches to the calculation of thermal conductivity have been examined. The approach discussed by Oligschleger and Schön,[14] and implemented in straight carbon nanotubes by Osman and Srivastava,[15] splits the nanotube into a series of equal "slabs" of atoms. Two of the slabs are thermally regulated to enforce a temperature gradient upon the system, as shown in Fig. 1. The temperature of each of these slabs is regulated by a scaling of the velocities of the atoms within the slab. The velocities are scaled according to

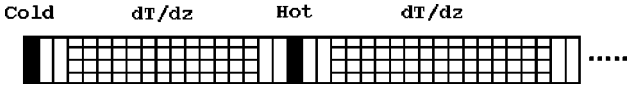

FIG. 1. Molecular dynamics setup for calculating the thermal conductivity of a straight carbon nanotube. The ellipses indicate that periodic boundary conditions are applied.

$$v_{i,\mathrm{new}} = v_{i,\mathrm{old}} \cdot \sqrt{\frac{T_{\mathrm{control}}}{T_{\mathrm{current}}}}, \tag{1}$$

where T_{control} is the desired temperature of the slab, and T_{current} is the current temperature. In this approach, $T_{\mathrm{control}} = T_{\mathrm{amb}} + \Delta T$ for the hot slab and $T_{\mathrm{control}} = T_{\mathrm{amb}} - \Delta T$ for the cold slab, where T_{amb} is the initial temperature of the solid. The change in energy of the controlled slabs at each time step is given by

$$\Delta E_{\mathrm{slab}} = \frac{1}{2} m \sum_{i=1}^{N} (v_{i,\mathrm{new}}^2 - v_{i,\mathrm{old}}^2), \tag{2}$$

where N is the number of atoms in the slab, m is the mass of each atom, and $v_{i,\mathrm{new}}$ is calculated according to Eq. (1). The heat flux density at the $n$thth time step of the simulation is calculated by taking an average of the net energy added at each previous time step

$$J(n) = \frac{1}{A} \cdot \frac{\sum_{j=1}^{n} |\Delta E_{\mathrm{hotslab}}(j) + \Delta E_{\mathrm{coldslab}}(j)|}{n \times \Delta t}, \tag{3}$$

where the $\Delta E_{\mathrm{slab}}(j)$ come from Eq. (2), Δt is the time associated with each simulation step, and A is the cross-sectional annular ring area of the nanotube.[15] After a large number of simulation steps, an equilibrium value of the heat flux density is obtained. The temperature gradient, dT/dz, is found by applying a linear fit to the temperatures of the slabs in the gray region in Fig. 1, and the thermal conductivity at the nth simulation step is the quotient of the heat flux density and the temperature gradient:

$$\mathrm{K}(n) = \frac{J(n)}{dT/dz}, \tag{4}$$

where $J(n)$ is given by Eq. (3). One final note that should be made from Fig. 1 is that periodic boundary conditions have been applied in order to eliminate edge effects.[14]

To investigate the thermal conductivity of the Y-junction nanotube, an algorithm similar to that described by Oligschleger and Schön has been chosen. The setup is similar to that shown in Fig. 1, except for the fact that, due to its linear asymmetry, periodic boundary conditions cannot be applied to the Y-junction configuration. Therefore, an alternate setup has been chosen, and can be seen in Fig. 2.

In this setup, the black slabs labeled "Fixed" have atoms that are fixed in space in order to prevent tube drift and oscillations during the simulation. The slabs labeled "Hot" and "Cold" are the velocity-scaled slabs, whose temperatures are controlled as described in Eq. (1). The energy flux density at the nth simulation step is calculated in the same manner as in Eq. (3), but with an extra term to account for the fact that there are two cold velocity-scaled slabs instead of just one

$$J(n) = \frac{1}{A} \cdot \frac{\sum_{j=1}^{n} |\Delta E_{\mathrm{hot}}(j) + \Delta E_{\mathrm{cold1}}(j) + \Delta E_{\mathrm{cold2}}(j)|}{n \times \Delta t}. \tag{5}$$

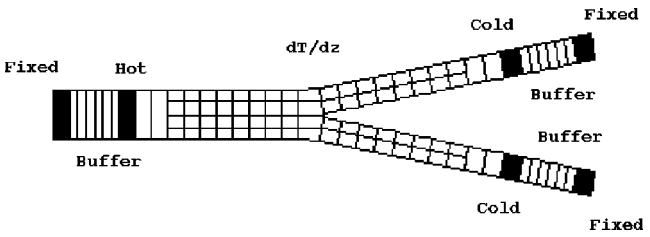

FIG. 2. Molecular dynamics setup for calculating the thermal conductivity of the Y-junction nanotube. The ends of the tube are fixed in space, the "Hot" and "Cold" slabs are thermally regulated through velocity scaling, and the buffer slabs act as a thermal shield against the tube ends.

The slabs labeled "buffer" act as thermal reservoirs, in an attempt to neglect edge effects by providing a buffer between the velocity-scaled slabs and the fixed tube ends. The temperature of these buffer slabs is the same as that of their adjacent velocity-scaled slabs. However, their temperature is maintained through a more realistic application of friction and random forces, which satisfy the fluctuation-dissipation theorem through the Langevin dynamics approach. In order to obtain a single temperature gradient dT/dx for the entire structure, the positions and temperatures of corresponding slabs in the two branches were averaged before a linear fit was calculated.

As stated earlier, the linear asymmetry of the Y-junction structure precludes the application of periodic boundary conditions to the system. The buffer slabs were added in an attempt to provide a shield from edge effects, but it is still possible that the tube ends could have an effect on the heat flow within the system. Thus, the proximity to edges could have an effect on the absolute magnitude of the thermal conductivity. This method, however, is reasonable for identifying trends and relative magnitudes of heat transport in a branched nanotube structure in comparison with straight nanotubes with or without defects.

III. RESULTS

For the MD simulations, a Y-junction with a (14,0) zigzag trunk splitting into two (7,0) zigzag branches was used. There were 35 slabs in each of the three branches, and one slab in the middle connecting them, for a total of 106 slabs including 3980 atoms. With a length of 4.26 Å per slab, each branch in the tube measured about 15 nm long. This is long enough for a qualitative comparison of thermal transport in branched and straight carbon nanotubes, but not for absolute values of thermal conductivity. The thermal conductivity simulation was run at base temperatures of 200 to 400 K in increments of 50 K. A temperature differential of ±50 K between the trunk and the two branches was used in each case. Two simulations were run for each base temperature, one with a hot trunk and cold branches (designated as "forward" heat flow), and one with a cold trunk and hot branches ("reverse" heat flow). For comparison, a (14,0) straight nanotube of 71-slab length was also run at these temperatures. The straight tube was configured in a manner similar to that shown in Fig. 2, with the fixed ends, buffer slabs, and

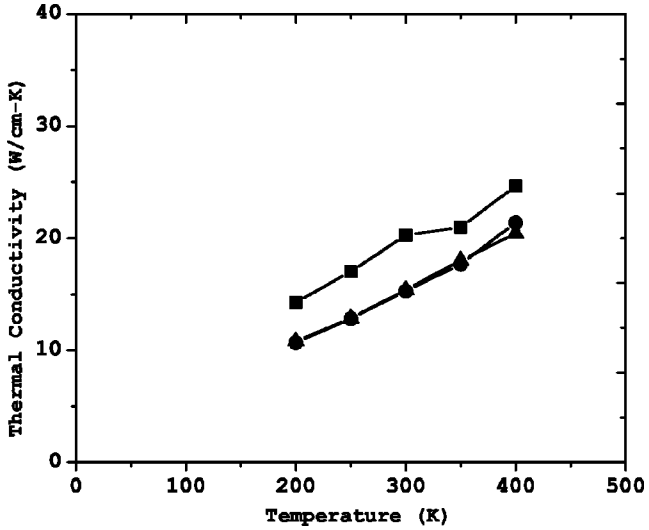

FIG. 3. Temperature dependence of the thermal conductivity. The squares represent the straight (14,0) nanotube, the triangles represent the forward heat flow configuration of the Y-junction tube, and the circles represent the reverse heat flow configuration of the Y-junction tube.

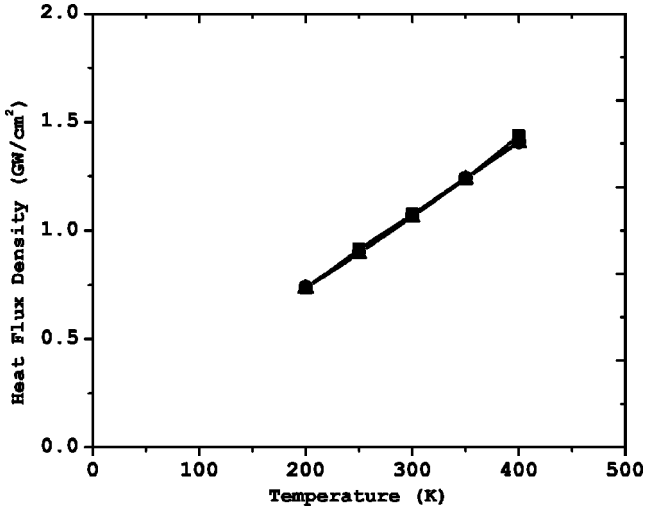

FIG. 4. Temperature dependence of the heat flux density. The squares represent the straight (14,0) nanotube, the triangles represent the forward heat flow configuration of the Y-junction tube, and the circles represent the reverse heat flow configuration of the Y-junction tube.

velocity-scaled slabs. Each simulation was run for 200 000 time steps, with the heat flux density averaged over the last 100 000 time steps. For these simulations, the time step was 0.5 fs, and the cross-sectional area was calculated based on an annular ring width of 3.4 Å.[15]

The results for the thermal conductivity of the nanotubes are summarized in Fig. 3. For temperatures up to 400 K, there is no significant difference between the "forward" and "reverse" heat conductivity of the Y-junction carbon nanotube. This is in contrast to the theoretical result indicating significant electrical rectification in the same Y-junction nanotube configuration.[11] Additionally, the thermal conductivity exhibits an increase with temperature similar to what has been reported experimentally[16] for straight carbon nanotubes. Figure 3 also indicates that the thermal conductivity of the straight (14,0) nanotube was consistently larger than that of the Y-junction structure.

The heat flux density results are shown in Fig. 4. This figure indicates that the forward and reverse energy flux values of the Y-junction nanotube are almost exactly the same for all temperatures. Furthermore, these flux values are essentially identical to those of the straight (14,0) nanotube. Given this, it stands to reason that the differences in thermal conductivity between the Y-junction and the straight nanotubes are due to differences in the temperature gradient. Figure 5 shows the values of the temperature gradient obtained, and indicates that the Y-junction tube has a higher temperature gradient than the straight (14,0) tube for all temperatures.

Figure 6(a) shows the temperature profile along the straight (14,0) nanotube at 300 K and Fig. 6(b) shows that of the Y-junction nanotube, also at 300 K. These figures help to explain the reason why the Y-junction nanotube has a higher temperature gradient than the straight nanotube. As seen in Fig. 6(b), the Y-junction nanotube exhibits a sharp discontinuity in the temperature profile at slab positions 35–37, where the trunk splits into the two branches. No such discontinuity in the temperature profile exists for the straight tube. This small region of the relatively large temperature gradient is a result of the presence of high resistance to heat flow at the junction. This high resistance, in turn, results in the lower values for the thermal conductivity of the Y-junction nanotube.

Discontinuities in the temperature profile have been observed in the context of MD simulations before. Using a nonequilibrium MD approach, Maiti, Mahan, and Pantelides[17] have investigated the heat flow across crystal grain boundaries. They have reported a similar temperature

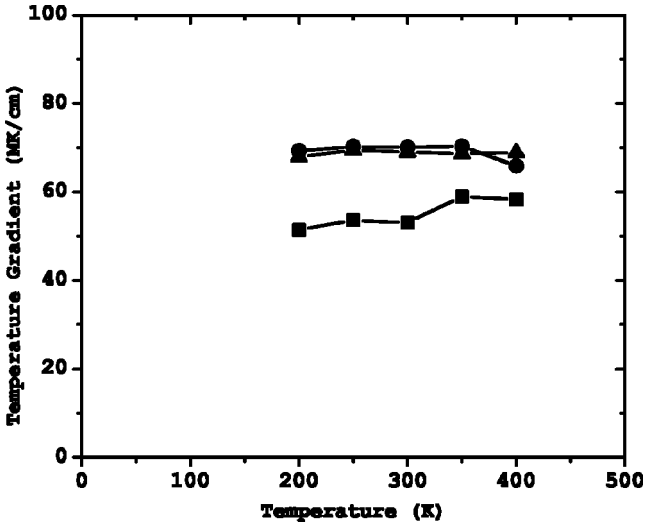

FIG. 5. Temperature dependence of the temperature gradient. The squares represent the straight (14,0) nanotube, the triangles represent the forward heat flow configuration of the Y-junction tube, and the circles represent the reverse heat flow configuration of the Y-junction tube.

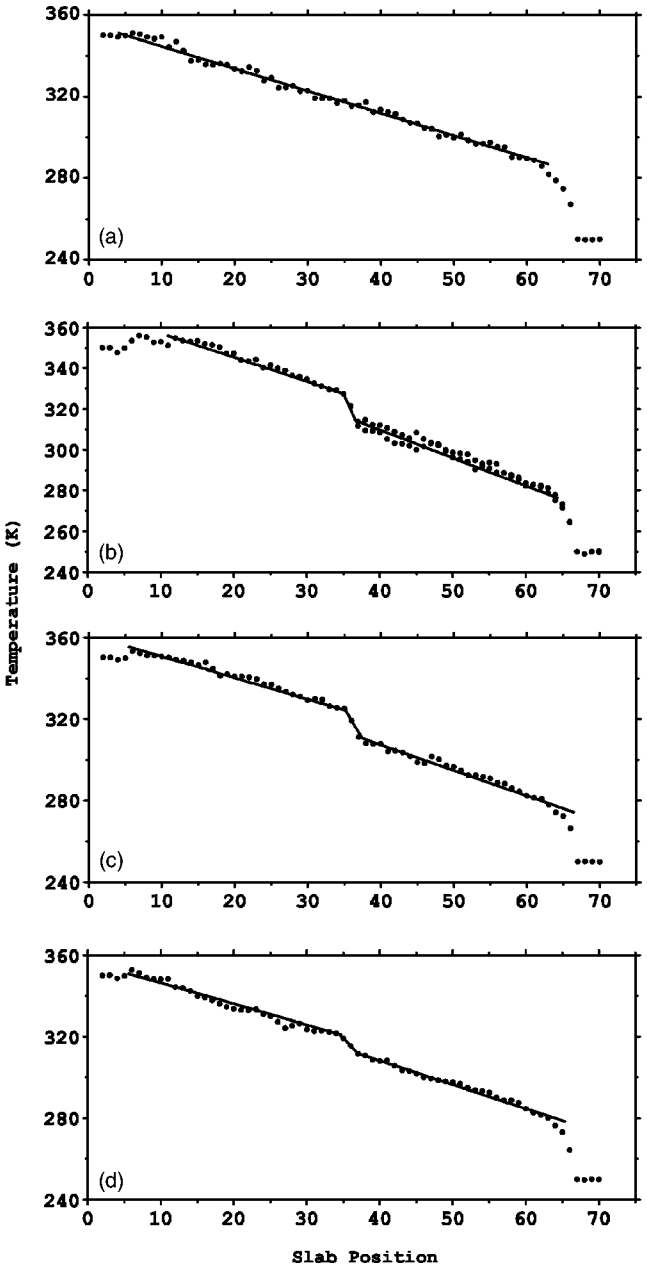

FIG. 6. Temperature profiles of (a) the straight (14,0) nanotube, (b) the Y-junction nanotube, (c) the straight (14,0) nanotube with vacancy defects, and (d) the straight (14,0) nanotube with a Stone-Wales (5,7,7,5) defect. Fit lines have been added to show the slope in each region.

profile across a grain boundary in a silicon crystal.[17] Maruyama, Taniguchi, and Shibuta have reported seeing a jump in the temperature profile of a carbon nanotube heterojunction consisting of a (12,0) tube connected to a (6,6) tube.[18] In each of these cases, the jump in the temperature profile seems to be associated with the presence of discontinuities or defects in the crystal lattice under investigation. These defects act as additional scattering centers and result in a region of large temperature gradient, which translates to a reduction in the thermal conductivity of the crystal. Che, Çağin, and Goddard have reported his type of behavior, with theoretical calculations that indicate an inverse relationship between the number of defects in a crystal and the thermal conductivity of the crystal.[19] In the Y-junction tube examined in this paper, lattice defects are present in the form of six heptagonal carbon rings at the junction point.[11]

In order to understand the origin of the discontinuity at the Y-junction, two types of defects were intentionally introduced into the middle of two straight (14,0) nanotubes. The first type of defect was in the form of atomic vacancies and was created by the removal of two atoms from the middle slab of the tube. The second type of defect was a Stone-Wales (5, 7, 7, 5) defect, where four hexagons are changed into two pentagons and two heptagons. These tubes were then run through the simulation at 300 K, with the usual ±50 K hot and cold slabs applied. The resulting temperature gradient of the tube with vacancies can be seen in Fig. 6(c), while that of the tube with the Stone-Wales defect can be seen in Fig. 6(d). As seen in these figures, the temperature profile of the straight nanotube with two vacancies is very similar to that of the Y-junction, while the temperature profile of the tube with the Stone-Wales defect exhibits a discontinuity that is much less pronounced. Additionally, the resulting values of the temperature gradient and the thermal conductivity of the (14,0) tubes with defects were calculated. The nanotube with vacancies had the same thermal conductivity and temperature gradient as those obtained for the Y-junction nanotube at the same temperature. The nanotube with the Stone-Wales defect had a smaller temperature gradient and thus a larger thermal conductivity than the Y-junction tube, but a smaller thermal conductivity than the defect-free (14,0) tube. Che *et al.* noted that Stone-Wales defects have a less significant effect on thermal conductivity than vacancies,[19] which is consistent with the smaller temperature profile discontinuity seen in Fig. 6(d). They concluded that the Stone-Wales defects were less severe because they do not change the bonding configuration of the lattice and thus induce less structural deformation. The greater amount of structural deformation in the Y-junction nanotube suggests that it will exhibit a more significant discontinuity in the temperature profile.

In an attempt to clarify the reason behind the presence of the jump in the temperature profiles, the phonon spectra of the nanotubes in question were investigated. The phonon spectra were found by taking the Fourier transform of the velocity autocorrelation functions of each tube, which were calculated over 1024 time steps in the MD simulations. Of interest were the frequency distributions of atomic vibrations along two different directions. Axial phonons and radial phonons represent vibrations parallel and perpendicular to the nanotube axis, respectively. Therefore, two autocorrelation functions were calculated, one using only the component of the atomic velocities parallel to the nanotube axis, and one using only velocity components perpendicular to the nanotube axis.

Figure 7(a) shows the axial phonon spectrum of the atoms in a single defect-free slab in the (14,0) nanotube. A primary peak exists at around 50 THz, with a lesser peak at about 20 THz. In Fig. 7(b), the axial phonon spectrum of the atoms in the slab with vacancies in the (14,0) tube is shown. Again, the phonon density peaks at about 20 and 50 THz. However, the magnitude of the 50 THz peak is about 15% smaller than

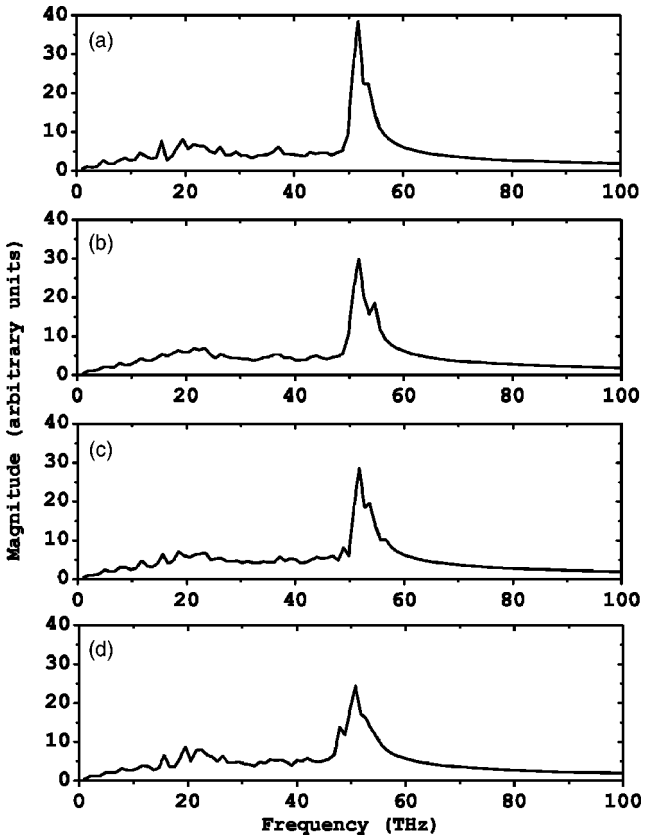

FIG. 7. Axial phonon spectra of (a) the straight (14,0) nanotube, (b) the straight (14,0) tube slab with vacancy defects, (c) the straight (14,0) nanotube slab with a Stone-Wales (5,7,7,5) defect, and (d) Y-junction slab 35. These spectra represent atomic vibrations parallel to the tube axis.

that of the defect-free slab. Figure 7(c) shows the axial phonon spectrum of the atoms in the slab with the Stone-Wales defect. The magnitude of the 50 THz peak is about 16% smaller than that of the defect-free slab. Finally, Fig. 7(d) shows the axial phonon spectrum of the atoms of slab 35 in the Y-junction tube. Slab 35 is the slab in the (14,0) trunk of the Y-junction that is adjacent to the middle "hub" slab. Moving from left to right along the temperature profile of the Y-junction tube in Fig. 6(b), one can see that slab 35 is where the first significant discontinuity in the temperature drop occurs. Again, peaks in the phonon density of the atoms in this slab exist at 20 and 50 THz. In this case the magnitude of the 50 THz peak is about 30% smaller than that in the defect-free (14,0) slab. Similar results were obtained for the radial phonon spectra of the nanotubes. The magnitudes of the 50 THz peaks in the radial phonon spectra of the Y-junction and (14,0) nanotube with vacancies were both 7% smaller than that of the defect-free (14,0) nanotube, while the peak in the tube with the Stone-Wales defect was 20% smaller.

IV. DISCUSSION

The steady state heat flow properties of a Y-junction nanotube consisting of a (14,0) trunk splitting into two (7,0) branches have been investigated using MD simulations. Thermal transport under steady state does not show any anisotropy with respect to the direction of the heat flow, which is in contrast to the evidence of electrical rectification in the same structure. In their calculations, Andriotis *et al.* accounted for the effects of quantum states on electrical conduction in Y-junction carbon nanotubes through an application of Green's function.[11] Recent experimentation has shown that the specific heat of carbon nanotubes increases linearly with temperature from 2 to 8 K, with an increase in the slope above 8 K.[20] This behavior implies a quantized one-dimensional phonon spectrum in carbon nanotubes at temperatures below 8 K. Above 8 K, the number of phonon modes excited becomes large enough to make the specific heat appear to be continuous with temperature. Therefore, quantum thermal effects are not seen at the temperatures used in these simulations. Furthermore, the use of Fourier's classical law of heat flow in the MD simulations precludes the inclusion of quantum thermal effects. Fourier's law provides an aggregate measure of the thermal conductivity by summing over all of the present phonon modes, but in doing so wipes out information about the contribution of individual phonons to heat flow. It has been demonstrated that the thermal conduction of carbon nanotubes at any temperature is dominated by phonons.[16] Therefore, it is possible that a more detailed model including a consideration of individual phonon modes may reveal thermal rectification in Y-junction nanotubes at very low temperatures.

The discontinuity in the temperature profile of the Y-junction nanotube seems to be the result of the discontinuous crystal structure present at the hub of the Y-junction. Similar temperature profiles have been observed in crystal grain boundaries,[17] junctions between nanotubes of different diameters,[18] and in single nanotubes with vacancy defects present. A study of the phonon modes in the investigated tubes indicates that the presence of defects reduces the density of axial and radial phonon modes. This connection between the temperature discontinuity and the atomic vibrations seems to indicate that both the axial and the radial modes are at least partly responsible for the transfer of heat along a nanotube, and that the interruption of these modes results in an interruption of heat transfer.

V. CONCLUSION

Using a MD simulation approach, the thermal conductivity of a Y-junction carbon nanotube at several temperatures has been calculated. These results indicate that no anisotropy of heat flow under equilibrium conditions occurs for this structure around room temperature. The sharp discontinuity in the temperature profile has been attributed to lattice discontinuities at the Y-junction. Phonon spectrum calculations have indicated that this discontinuity in the crystal lattice inhibits atomic vibrations both parallel and perpendicular to the tube axis.

ACKNOWLEDGMENTS

Part of this work (A.C.) was supported through a NASA Ames Education Associates summer internship provided by DS from a DDF (2001-2003) grant at ARC. A part of this work (D.S.) acknowledges the support by NASA Ames contract NAS2-03144 to UARC.

*Email address: acumming@eecs.wsu.edu
†Email address: osman@eecs.wsu.edu

[1] S. Iijima, Nature (London) **354**, 56 (1991).
[2] R. Saito, M. Fujita, G. Dresselhaus, and M. S. Dresselhaus, Phys. Rev. B **46**, 1804 (1992).
[3] N. Hamada, S. I. Sawada, and A. Oshiyama, Phys. Rev. Lett. **68**, 1579 (1992).
[4] M. Menon and D. Srivastava, Phys. Rev. Lett. **79**, 4453 (1997).
[5] M. Menon and D. Srivastava, J. Mater. Res. **13**, 2357 (1998).
[6] D. Srivastava, M. Menon, and P. M. Ajayan, J. Nanopart. Res. **5**, 395 (2003).
[7] L. Jing, C. Papadopolous, and J. Xu, Nature (London) **402**, 253 (1999).
[8] C. Papadopoulos, A. Rakitin, J. Li, A. S. Vedeneev, and J. M. Xu, Phys. Rev. Lett. **85**, 3476 (2000).
[9] M. Terrones, F. Banhart, N. Grobert, J.-C. Charlier, H. Terrones, and P. M. Ajayan, Phys. Rev. Lett. **89**, 075505 (2002).
[10] A. N. Andriotis, M. Menon, D. Srivastava, and L. Chernozatonskii, Phys. Rev. Lett. **87**, 066802 (2001).
[11] A. N. Andriotis, M. Menon, D. Srivastava, and L. Chernozatonskii, Phys. Rev. B **65**, 165416 (2002).
[12] J. Tersoff, Phys. Rev. Lett. **61**, 2879 (1988).
[13] D. W. Brenner, Phys. Rev. B **42**, 9458 (1990).
[14] C. Oligschleger and J. C. Schön, Phys. Rev. B **59**, 4125 (1999).
[15] M. Osman and D. Srivastava, Nanotechnology **12**, 21 (2001).
[16] J. Hone, M. Whitney, C. Piskoti, and A. Zettl, Phys. Rev. B **59**, R2514 (1999).
[17] A. Maiti, G. Mahan, and S. Pantelides, Solid State Commun. **102**, 517 (1997).
[18] S. Maruyama, Y. Taniguchi, and Y. Shibuta, *Eurotherm 75*, Champagne (2003).
[19] J. Che, T. Çağin, and W. Goddard III, Nanotechnology **11**, 65 (2000).
[20] J. Hone, B. Batlogg, Z. Benes, A. Johnson, and J. Fischer, Science **289**, 1730 (2000).